Thermal Unfolding of a Group I Ribozyme: The Low-Temperature Transition Is Primarily Disruption of Tertiary Structure†

Aloke Raj Banerjee, John A. Jaeger, and Douglas H. Turner*

Department of Chemistry, University of Rochester, Rochester, New York 14627-0216

Received July 17, 1992; Revised Manuscript Received October 16, 1992

ABSTRACT: Little is known about the folding pathways of RNA. A particularly interesting RNA is L-21 Sca I, a linear form of the self-splicing intron from the precursor of the *Tetrahymena thermophila* large subunit (LSU) rRNA. Thermal unfolding of L-21 Sca I is studied by UV absorption and chemical mapping in 50 mM Na^+ and 10 mM free Mg^{2+} at pH 7.5. UV melting experiments identify two major transitions with maxima at 65 and 73 °C. Chemical mapping at the beginning and middle of the first transition suggests it primarily involves disruption of tertiary structure. Phylogenetic comparisons suggest a potential tertiary interaction between loops L2.1 and L9.1a. Chemical mapping and melting experiments on a truncated form of the intron lacking P9.1a, L-21 Nhe I, are consistent with this hypothesis. The results indicate that increasing temperature disrupts tertiary interations before disrupting secondary structure. This suggests tertiary interactions are weaker than secondary interactions in this case. These results support an important assumption for RNA structure prediction: that secondary structure dominates the free energy of folding.

The importance of the RNA folding problem has increased with the rapidly expanding data base of RNA sequences (Olson et al., 1989; Stephens et al., 1990; Mitsuya et al., 1990) and with the development of therapeutics targeting RNA (Uhlmann & Peyman, 1990). This is because an understanding of RNA folding will provide a foundation for prediction of RNA structure from sequence (Turner et al., 1988). Surprisingly, the steps in folding RNA have only been studied in detail for tRNAs (Crothers et al., 1974; Riesner & Römer, 1973; Hilbers et al., 1976; Rhodes, 1977), viroids (Riesner, 1987; Steger et al., 1984), and 5S rRNA (Kjems et al., 1985). It is unlikely, however, that all RNA motifs are represented in those cases. For example, viroids are thought to have no significant tertiary interactions (Riesner, 1987; Steger et al., 1984). The self-splicing LSU rRNA intron from *Tetrahymena thermophila* contains many secondary and tertiary structural motifs not represented in tRNAs or mature viroids (Michel & Dujon, 1983; Burke et al., 1987; Kim & Cech, 1987; Michel & Westhof, 1990). Thermal melting of a circular and a linear (L-19) form of this intron occurs in two main transitions (Jaeger et al., 1990a). Another linear form of this intron, L-21 Sca I, has been developed which catalyzes cleavage and ligation reactions between RNAs (Zaug et al., 1988). In this paper, the thermal unfolding of L-21 Sca I is studied by UV absorption and chemical mapping (Peattie, 1979; Inoue & Cech, 1985; Moazed et al., 1986; Ehresmann et al., 1987).

The UV melting experiments identify two major transitions. Chemical mapping and melting experiments on L-21 Sca I and a truncated form, L-21 Nhe I, suggest the lowest temperature transition primarily involves disruption of tertiary structure. The results suggest tertiary interactions are weaker than secondary structure interactions in this case. This supports a common assumption in algorithms for predicting secondary structures of RNA (Zuker, 1989; Turner et al., 1988) and suggests that chemical mapping results at elevated temperatures can provide useful constraints for predictions of secondary structure.

† Supported by NIH Grant GM22939.

* Author to whom correspondence should be addressed.

MATERIALS AND METHODS

Ribozymes. L-21 Sca I and L-21 Nhe I ribozymes were prepared by T7 RNA polymerase transcription of pT7L-21 plasmid cut with Sca I and Nhe I endonucleases, respectively (Zaug et al., 1988). Each RNA was purified by polyacrylamide gel electrophoresis on a 4% polyacrylamide 7 M urea gel. The RNA was visualized by UV shadowing and eluted into 0.1% SDS, 0.1 mM Na_2 EDTA, and 40 mM ammonium acetate at pH 8.0 by the crush and soak method (Barfod & Cech, 1988). After elution, the ribozyme was run through a Sephadex G-50 column, precipitated in ethanol, and stored at –20 °C in sterile water.

In principle, the L-21 Sca I and L-21 Nhe I transcripts could react in transesterification reactions because roughly 9% of L-21 Sca I (Zaug et al., 1988) and most of L-21 Nhe I (Barfod & Cech, 1988) have a 3′-terminal G that can function as a nucleophile (Joyce & Inoue, 1989). The chemical stabilities of body labeled transcripts were therefore tested by incubating them in melting buffer for up to 30 min at 50 °C and 11 min at 65 °C and running the products on a 4% polyacrylamide denaturing gel. Only a single band was observed for L-21 Sca I. For L-21 Nhe I at 50 °C, minor bands were also observed. These bands were excised and quantified by scintillation counting. At 50 °C, the total increase in ^{32}P in the minor bands upon incubation was less than 4% of the ^{32}P in the L-21 Nhe I band. Thus both transcripts are chemically stable.

Oligonucleotides. Primers were prepared by the phosphoramidite method (Beaucage & Caruthers, 1981; Matteuchi & Caruthers, 1981; Barone et al., 1984) and then purified by high-performance liquid chromatography and stored at –20 °C in sterile water. Extinction coefficients were estimated with the nearest neighbor model (Richards, 1975). The sequences of the primers and their extinction coefficients at 260 nm (M^{-1} cm^{-1}) are as follows: IP70 (AACCGATGCAATCTAT), 1.59×10^5; IP141 (AAGTTTCCCCTGAGAC), 1.60×10^5; IP274 (CATCTTCCCCGACCG), 1.31×10^5; IP315 (CTCCCATTAAGGAGAGG), 1.01×10^5; IP350 (GCGGCTCCAGTGTTG), 1.38×10^5; IP395 (ACTCCAAAACTAATCA), 7.88×10^4. Primers were 5′-

0006-2960/93/0432-153$04.00/0

Table I. Rates of Reaction between Chemical Modification Reagents and Monomers at Various Temperatures, and Concentrations and Times for Reaction with Ribozymes

		reaction with 5'NMP					reaction with ribozymes	
reagent	temp (°C)	5'NMP	[5'NMP] (mM)	[reagent] (mM)	pseudo-first-order rate constant (min^{-1})	second-order rate constant (M^{-1} min^{-1})	[reagent] (mM)	reaction time (min)
CMCT	0	U			(0.0014)[a]	(0.014)[a]	40.5	90
	50	U	10	100	0.012	0.12	40.5	0.50
	65	U	10	100	0.025	0.25	40.5	0.25
	80					(0.372)[a]	40.5	0.12
	0	G			(1.8×10^{-4})[a]	(0.0044)[a]	40.5	90
	50	G	0.1	40.5	0.016	0.40	40.5	0.50
	65	G	0.1	40.5	0.053	1.31	40.5	0.25
	80					(3.63)[a]	40.5	0.12
kethoxal	0	G			(0.046)[a]	(2.4)[a]	19	180
	50	G	0.1	0.76	0.42	553	0.76	8.3
	65	G	0.1	0.76	1.27	1670	0.76	2
	80					(6316)[a]	0.76	0.5
DMS	0						60	90
	50	A	$\sim 10^{-9}$	60	(0.038)[b]	(0.64)[b]	60	0.17
	65	A	$\sim 10^{-9}$	60	(0.059)[b]	(0.99)[b]	60	0.08
	80					(1.20)[a]	30	0.08
DEPC	0						650	180
	50						650	25
	65						650	6

[a] Extrapolated with the Arrhenius equation, $k = A \exp(-E_a/RT)$. [b] Not a true rate constant due to instability of DMS in melting buffer.

end labeled with [γ-^{32}P]ATP from New England Nuclear and T4 polynucleotide kinase obtained from New England Biolabs.

Reagents and Enzymes. The modification reagents were 1-cyclohexyl-3-(2-morpholinoethyl)carbodiimide metho-*p*-toluenesulfonate (CMCT) and diethyl pyrocarbonate (DEPC) from Sigma, dimethyl sulfate from Aldrich, and kethoxal (β-ethoxy-α-ketobutyraldehyde) from Upjohn. The buffer, 4-(2-hydroxyethyl)-1-piperazineethanesulfonic acid (HEPES), was from Aldrich. Nuclease P1 was from Sigma, and avian myeloblastosis virus reverse transcriptase was from Life Sciences Incorporated. The deoxyribo-, dideoxyribo-, and ribonucleoside triphosphates were from Pharmacia. Gel solutions were prepared from ultrapure acrylamide, *N,N'*-methylene-bis-acrylamide, and boric acid from Bio-Rad. 5'-Guanosine monophosphate (5'GMP), 5'-uridine monophosphate (5'UMP), and 3'-adenosine monophosphate (3'AMP) were from Sigma.

Optical Melting Curves. Absorbance vs temperature melting curves were primarily measured at 260 and 280 nm in 80 mM HEPES (made with 40 mM Na^+ salt and 40 mM free acid) at pH 7.5, 10.5 mM $MgCl_2$, 0.5 mM Na_2EDTA, and 10 mM NaCl (melting buffer) with a heating rate of 0.5 °C min^{-1} on a Gilford 250 spectrophotometer interfaced to a Zenith 250 computer. For L-21 Sca I, a heating rate of 0.25 °C min^{-1} gave the same melting curve as 0.5 °C min^{-1}, but a heating rate of 1 °C min^{-1} resulted in precipitation of the RNA at about 65 °C. Derivatives of the melting curves were taken with a seven-point parabolic fit with binomial weighting at each temperature (Bevington, 1969).

Stability of Modification Reagents and Reactivity with Mononucleotides. As a guide for choosing reaction times for chemical modification of ribozyme, the stabilities of modification reagents reacting at Watson–Crick pairing position and the kinetics of their reactions with mononucleotides were studied as a function of temperature. Mononucleotide solutions were preincubated for 5 min at the desired temperature before addition of modification reagent. The experiments are described below and the results are summarized in Table I.

CMCT. The stability of CMCT in melting buffer made up in 99.9 atom % D_2O was monitored by NMR. At 65 and 50 °C, respectively, no changes were observed in chemical shift or amplitude over 1- and 12-h periods. Evidently, CMCT is stable in this buffer.

Reaction of 10 mM 5'UMP with 100 mM CMCT at 65 and 50 °C in melting buffer was followed by thin layer chromatography (TLC) on silica gel plates (Baker Si250F). At desired time intervals, aliquots were streaked onto the plate and dried. Plates were developed in *n*-butanol/glacial acetic acid/water 5:2:3 (v/v/v). Reactant and product bands were scraped off and eluted in 1 mL of water. Absorbances at 260 nm were then measured. Fraction reaction was defined as $F = A_p/(A_R + A_p)$, where A_p and A_R are absorbances for product and reactant bands, respectively. This assumes the extinction coefficients for product and reactant are the same. Pseudo-first-order rate constants, k', were calculated by fitting the data to

$$F_t = F_\infty(1 - e^{-k't}) \quad (1)$$

Here F_t is the fraction reacted at time t, and F_∞ is the fraction reacted at equilibrium. The second-order rate constant was calculated as $k = k'/[\text{CMCT}]$. Kinetic plots are shown in supplementary material (see paragraph at end of paper regarding supplementary material), and second-order rate constants are listed in Table I. Reaction at 65 °C is roughly twice as fast as at 50 °C. Extrapolation of the results to 23 °C gives $k = 0.04$ M^{-1} min^{-1}, slightly slower than the value of 0.073 M^{-1} min^{-1} reported previously (Girshovich et al., 1968).

The reactivity of 0.1 mM 5'GMP with 40.5 mM CMCT at 65 and 50 °C in melting buffer was followed directly by monitoring absorbance at 290 nm (Girshovich et al., 1968). The reference cell contained all components of the reaction mixture except 5'GMP. Kinetic plots are shown in supplementary material. Rate constants derived as described above are listed in Table I. Reaction at 65 °C is roughly three times

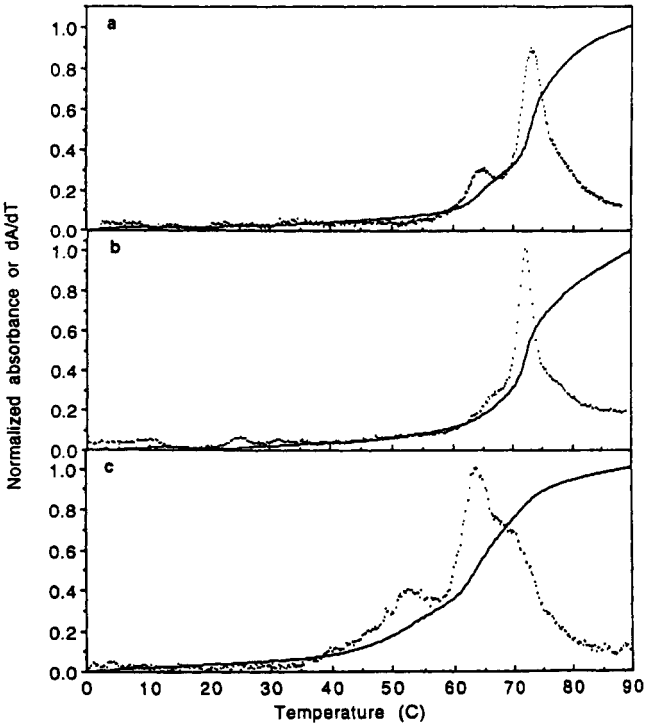

FIGURE 1: Melting curves (solid lines) and their derivatives, dA/dT, (dotted lines) for ribozymes measured at 280 nm at a heating rate of 0.5 °C min^{-1}. (a) L-21 Sca I in melting buffer (10.5 mM Mg^{2+}). (b) L-21 Nhe I in melting buffer (10.5 mM Mg^{2+}). (c) L-21 Sca I in melting buffer except that [Mg^{2+}] = 1.5 mM.

as fast as at 50 °C. Extrapolation of the results to 23 °C gives k = 0.04 M^{-1} min^{-1}, in good agreement with the value of 0.047 M^{-1} min^{-1} reported previously (Girshovich et al., 1968).

DMS. The stability of 60 mM DMS in melting buffer made up in 99.9 atom % D_2O was monitored by NMR. The half-lives for hydrolysis of DMS at 65 and 50 °C are 6 and 1 min, respectively.

The instability of DMS in melting buffer precludes a simple pseudo-first-order study of its reaction with mononucleotides. Apparent pseudo-first-order rate constants were therefore calculated by measuring the time required for 5% of ^{32}P-labeled 5′AMP to react with DMS. Labeled 5′AMP was prepared by 5′ labeling 3′AMP with [γ-^{32}P]ATP, removing the 3′-phosphate with P1 nuclease (Bass & Weintraub, 1988), and purifying 5′AMP by TLC on silica gel plates (Baker Si250F). Reaction with an initial concentration of 60 mM DMS was monitored by taking aliquots at desired times, streaking them on silica gel plates, and developing the plates in isopropyl alcohol/ammonium hydroxide/water 6.5:1:2.5 (v/v/v). Bands were located by autoradiography and quantitated by counting in Ecosinct A scintillation fluid in a Packard Tri-Carb 4530 scintillation counter. Kinetic plots are shown in the supplementary material. The time required for 5% reaction was 52 and 80 s at 65 and 50 °C, respectively. Apparent pseudo-first order rate constants were calculated from these times and eq 1 by assuming F_∞ = 1. These were then converted to the apparent second-order rate constants that are listed in Table I. Equivalent experiments were attempted with ^{32}P-labeled 5′ CMP, but the reaction was too slow to monitor relative to degradation of DMS.

Kethoxal. The stability of kethoxal was monitored by following the absorbance at 295 nm of a 0.76 mM kethoxal solution. In melting buffer, the half-life for disappearance of kethoxal was 75 min at 65 °C and even longer at 50 °C.

The reaction of kethoxal with 0.1 mM 5′GMP in melting buffer at 65 and 50 °C was followed by monitoring absorbance at 270 nm (Litt & Hancock, 1967). Kethoxal reacts with GMP much faster than it decays in the absence of GMP. Kinetic plots are shown in the supplementary material. Plots were analyzed as described for CMCT to give pseudo-first-order and then second-order rate constants (Table I).

Chemical Mapping Experiments. Ribozymes in 25 μL of melting buffer were reacted with modification reagent at 0, 50, and 65 °C in a Lauda RC6 bath. Aliquots of 10 pmol of L-21 Sca I or L-21 Nhe I ribozymes were modified separately with each of the four modification reagents. Typically, the 10 pmol was dissolved in 24 μL of melting buffer to give a concentration of 0.4 μM. Ribozymes were then preincubated for 45 min at 0 °C or 5 min at 50 °C or 5 min at 65 °C. For DMS, 1 μL of 1.5 M DMS in ethanol was then added to the ribozyme. For DEPC, 2.5 μL of neat DEPC was added to the ribozyme. For kethoxal, 2.5 μL of 0.2 M kethoxal in 20% ethanol was added. In case of CMCT modification, 10 pmol of the ribozyme was dissolved in 12.5 μL of melting buffer. After preincubation, 12.5 μL of the same buffer containing 81 mM CMCT and preequilibrated at the desired temperature was added. All modification reagent solutions were prepared on ice immediately before reaction. Table I lists final concentrations of modification reagents and the reaction times.

Conditions were chosen to give observable modification patterns while retaining significant full-length extension of reverse transcripts to assure less than one modification per molecule. For DMS and kethoxal, modification times at 50 °C are about 40% longer than suggested by studies on mononucleotides (see Table I). Thus positions of enhanced reactivity at 65 °C are conservatively estimated. For DEPC, studies in the literature suggest incubation times at 50 °C should be between 2 and 5 times longer than at 65 °C (Kjems et al., 1985; van Belkum et al., 1988; de Bruijn & Klug, 1983; Wyatt et al., 1990). The factor of 4 chosen here falls within this range. For all reagents, several regions of L-21 Sca I were probed at a variety of modification times and reagent concentrations without any change in the pattern observed. Previous studies on a circular form of the ribozyme, CIVS, at 0 °C gave little modification for reaction times suggested by extrapolation of the kinetics in Table I (Jaeger, 1989). Thus, the relatively long reaction times previously chosen for CIVS were used for studies at 0 °C (Jaeger et al., 1990a).

Modification reactions were stopped by adding 10 μg of bulk tRNA (Sigma) and 0.3 M sodium acetate at pH 7.0, except for kethoxal where 0.2 M potassium borate at pH 7.5 was added in addition to tRNA and sodium acetate to stabilize the kethoxal adduct (Litt, 1969; Stern et al., 1988). The RNA was then precipitated with 3 volumes of 99% ethanol. After centrifugation, pellets were washed with 70% ethanol and redissolved at a concentration of 1 pmol/μL in sterile water.

Modifications were detected by reverse transcription (Inoue & Cech, 1985; Moazed et al., 1986). Primer (0.6 pmol) labeled with ^{32}P at the 5′-end was annealed to 1 pmol of modified ribozyme by following the procedure of Moazed et al. (1986). Control lanes for each reagent contained samples treated identically except that no modification reagent was added. To identify the modified bases, four sequencing lanes were run. The samples in these lanes were generated by reverse transcription in the presence of 0.1 mM ddATP, ddCTP, ddGTP, or ddUTP. For analysis, samples were loaded onto 0.4 mm × 45 cm, 10% acrylamide (1:30 bis/acrylamide), 7 M urea gels and electrophoresed for 2–4 h at a constant power of 60 W in running buffer of 100 mM Tris borate and 2 mM Na_2EDTA at pH 8.0.

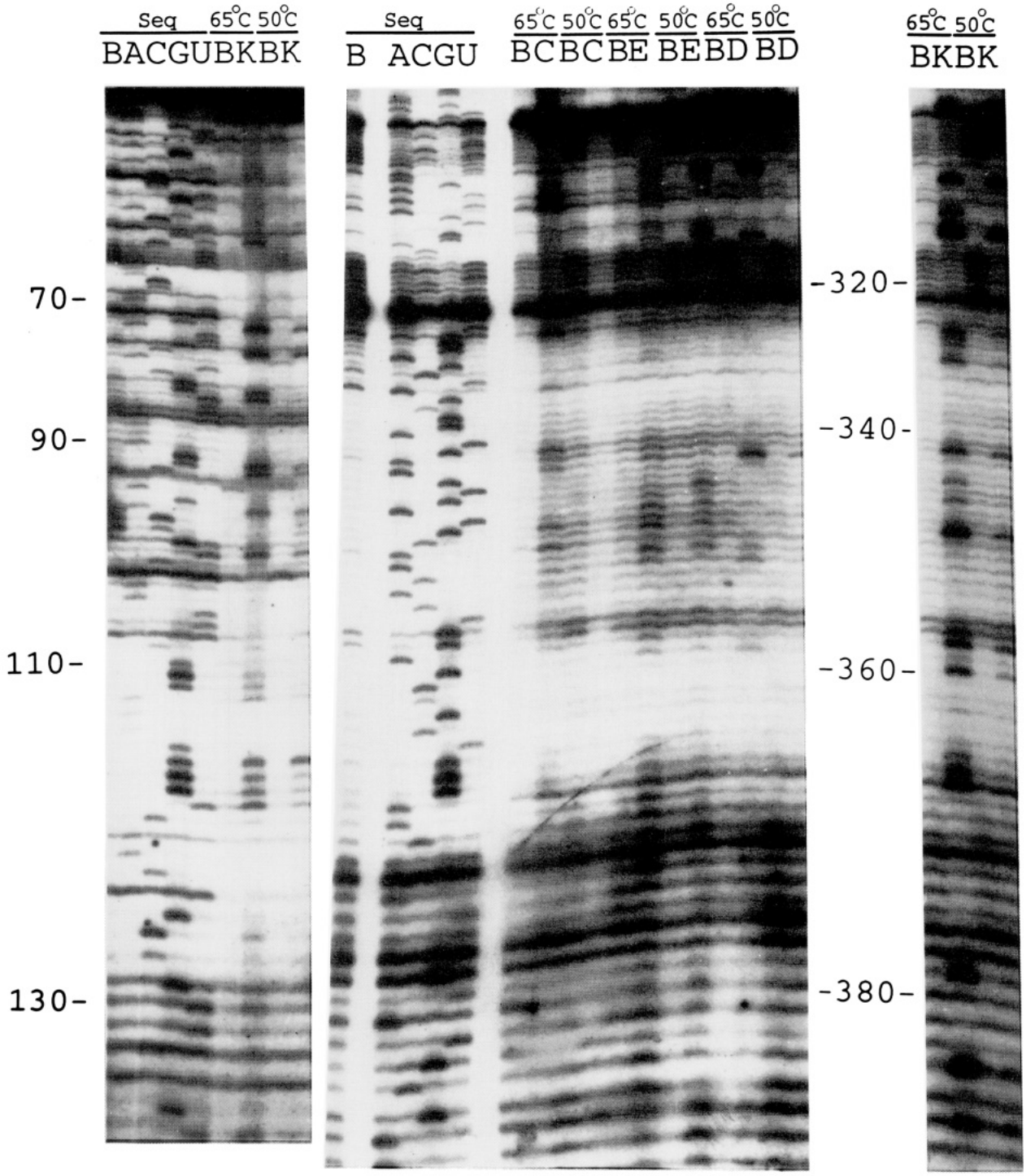

FIGURE 2: Autoradiograms of a sequencing gel of L-21 Sca I in melting buffer at 65 and 50 °C. Abbreviations: (B) blank control lane to the immediate left of its corresponding experimental lanes; (A, C, G, U) sequence lanes. (a, left) Guanosines near the 5′-end of L-21 Sca I probed with kethoxal using primer IP 141. (b, right) Probing of bases at the 3′-end of ribozyme with CMCT (C), DEPC (E), DMS (D), and kethoxal (K) using primer IP 395. Note that the extension of reverse transcriptase is 3′ to 5′ of the RNA and falls off one base 3′ to a modified base.

Computer Prediction and Prediction of Melting Temperatures for Hairpins. Secondary structures were predicted with the program of Zuker (Zuker, 1989; Jaeger et al., 1990b) as modified by Jaeger et al. (1990a) for calculations at any temperature. Thermodynamic parameters were those reported by Freier et al. (1986), Turner et al. (1988), Jaeger et al. (1989), and He et al. (1991). The same thermodynamic parameters were used to predict melting temperatures, T_M's, for hairpins in the phylogenetic secondary structure. Terminal GU pairs and unpaired nucleotides at the free 3′-end of the stem were included in the calculations.

RESULTS

Optical Melting of Ribozymes. Thermal unfolding of the ribozymes, L-21 Sca I and L-21 Nhe I, was followed by measuring absorbance vs temperature (see Figure 1). At 10 mM free Mg^{2+}, there is little change in absorbance below 50 °C. For L-21 Sca I, two transitions are observed above 50 °C. These give rise to maxima at 65 and 73 °C in the differential melting curve. For L-21 Nhe I, only one major transition is observed, giving rise to a maximum at 72 °C in the differential melting curve. At 1 mM free Mg^{2+}, transitions

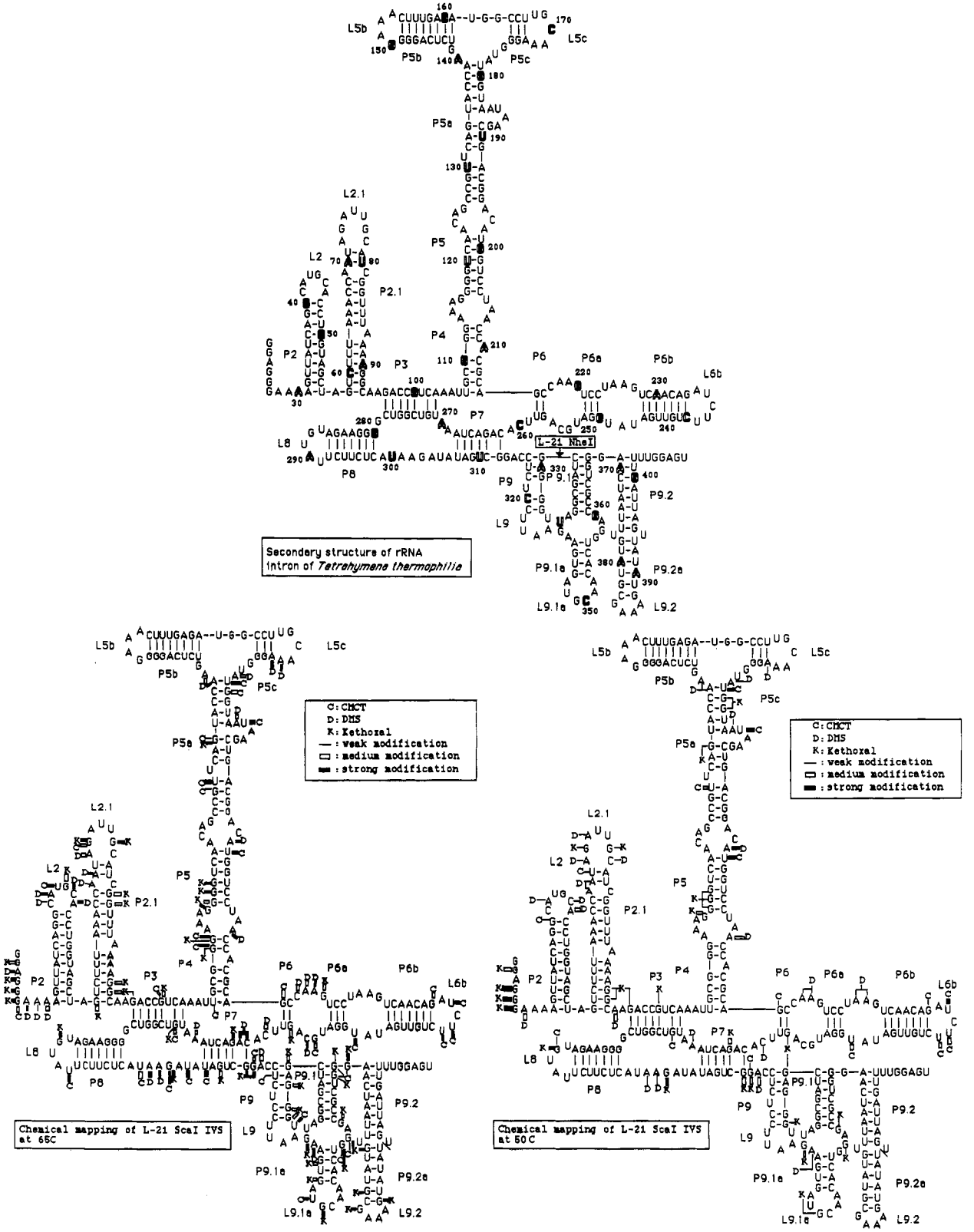

FIGURE 3: (a, top) Phylogenetic secondary structure of ribozymes with numbering and nomenclature based on the complete excised intron (Michel & Dujon, 1983; Burke et al., 1987). Every tenth nucleotide has been outlined and numbered. Chemical mapping data on L-21 Sca I for the Watson–Crick base pairing positions in melting buffer are shown at (b, bottom left) 65 °C and (c, bottom right) 50 °C. Symbols show strong (solid rectangles), medium (open rectangles), or weak (—) modification by CMCT (C), DMS (D), or kethoxal (K). The slash between nucleotides 393 and 394 represents the 3′-end of the 3′-terminal primer.

are observed for L-21 Sca I at 53, 63, and 70 °C (see Figure 1c).

Chemical Modification of Ribozymes. Modification times at different temperatures (Table I) were chosen on the basis of the kinetics of monomer reactivity discussed under Materials and Methods and listed in Table I. Typical autoradiograms of gels from chemical modification experiments are shown in Figure 2. Results of the mapping experiments at 50 and 65 °C are presented in Figures 3–6. Results at 0 °C are shown in supplementary material. Stops in the sample lanes, which were also present in the control lanes, have not been included. Most regions that are base-paired in the phylogenetic structure

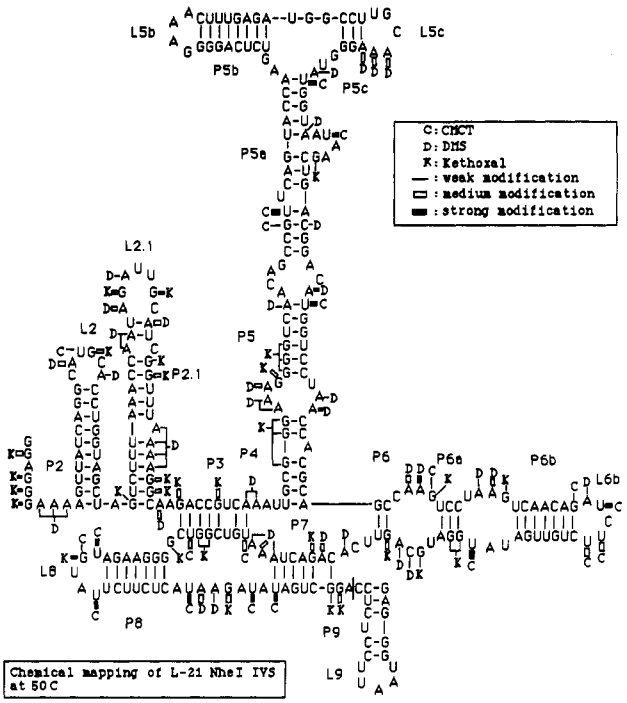

FIGURE 4: Chemical mapping data on L-21 Nhe I for the Watson–Crick base-pairing positions in melting buffer at 50 °C. Symbols show strong (solid rectangles), medium (open rectangles), or weak (—) modification by CMCT (C), DMS (D), or kethoxal (K). The slash between nucleotides 314 and 315 represents the 3′-end of the 3′-terminal primer.

are not attacked by the modification reagents. Many unpaired nucleotides, however, are also unreactive. This suggests that tertiary interactions and folding protect unpaired nucleotides.

Modification of L-21 Sca I Ribozyme. At 65 °C, strong hits at Watson–Crick pairing positions are observed at 47 nucleotides of L-21 Sca I. The only strong hit at a nucleotide that is paired in the phylogenetic structure and not adjacent to unpaired nucleotides is at G382. G382 is in a GU pair and thus potentially reactive even when paired, since the G amino group is not hydrogen bonded. Evidently, the phylogenetic secondary structure is intact at 65 °C.

At 50 °C, strong hits at Watson–Crick pairing positions are observed at only 10 nucleotides of L-21 Sca I (Figure 3). All are consistent with the phylogenetic secondary structure in that the strongly modified nucleotides are either unpaired or adjacent to unpaired nucleotides.

L-21 Sca I was also mapped at 0 °C. Twenty strong hits at Watson–Crick pairing positions were observed, all consistent with the phylogenetic secondary structure (see supplementary material).

At 80 °C, only the 3′-end of L-21 Sca I was mapped. Between nucleotides 312 and 393, 28 strong hits are observed, some of which occur in the middle of helixes (see supplementary material). Evidently, the secondary structure is disrupted at 80 °C, as expected from the melting curve.

Modification of L-21 Nhe I Ribozyme. At 50 °C, strong hits at Watson–Crick pairing positions are observed at 20 nucleotides of L-21 Nhe I (Figure 4). All are consistent with the phylogenetic secondary structure, and nine are identical to strong hits observed with L-21 Sca I at 50 °C. Evidently, deleting the 78 nucleotides at the 3′-end of the molecule does not result in a rearrangement of secondary structure but does expose previously unreactive nucleotides. Nine of the 11 new strongly modified nucleotides are also strongly modified in L-21 Sca I at 65 °C, and another is moderately modified. The only nucleotide strongly modified in L-21 Nhe I at 50 °C and not strongly or moderately modified in L-21 Sca I at 65 °C is U287.

L-21 Nhe I was also mapped at 0 °C using the same reaction times as with L-21 Sca I. Twenty-four strong hits at Watson–Crick pairing positions are observed, all consistent with the phylogenetic secondary structure (see supplementary material).

Computer Prediction of Structure. The secondary structures of L-21 Sca I and L-21 Nhe I were predicted at 0, 50, and 65 °C, with and without the seven base pairs of P3 forced. Foldings for L-21 Sca I at 65 and 50 °C are shown in Figure 7. Foldings for L-21 Nhe I were similar.

DISCUSSION

Two transitions are observed in the melting of L-21 Sca I at 10 mM Mg^{2+}, as previously observed for the circular and L-19 forms of this intron (Jaeger et al., 1990a). The transition centered at 73 °C presumably disrupts essentially all secondary structure. Here secondary structure is defined as base pairing that can be represented by nonintersecting chords across a circle around which the sequence is written (Zuker & Sankoff, 1984; Nussinov et al., 1978). The temperature range observed for disruption of secondary structure is roughly consistent with melting temperatures predicted for most of the hairpins in the secondary structure. For example, using available parameters (Freier et al., 1986; Turner et al., 1988; Groebe & Uhlenbeck, 1988; He et al., 1991) and approximating a GA_3 loop by GCAA (SantaLucia et al., 1992), predicted T_M's for P2.1, P5b, P6b, P8, P9, P9.1, and P9.2 are 70, 71, 78, 77, 78, 81, and 73 °C, respectively. Only P2 with a predicted T_M of 90 °C is expected to melt outside the range observed.

The structural change responsible for the lower temperature transition was probed by chemical mapping at the midpoint of the transition, 65 °C, giving 47 strong hits (Figure 3b). Assuming it is possible to modify base pairs adjacent to unpaired nucleotides, only the strong hit at G382 is not consistent with the phylogenetic secondary structure. G382 is involved in a GU pair and thus may be reactive even when paired. Thus, of the 37 new strong hits induced by raising the temperature from 50 to 65 °C, none is clearly consistent with disruption of secondary structure. This suggests the transition at 65 °C is mainly due to disruption of tertiary structure.

Figure 8a highlights nucleotides whose reactivity at Watson–Crick pairing positions changes by at least two levels between 65 and 50 °C (e.g., strongly to weakly modified). Eight of the 25 new strong hits are between nucleotides 342 and 388, suggesting that interactions involving the 3′-end of L-21 Sca I are particularly temperature sensitive. This region is deleted in the L-21 Nhe I transcript (Barfod & Cech, 1988). As shown in Figure 1, the low-temperature transition present in the melting curve of L-21 Sca I is almost absent in L-21 Nhe I, consistent with the hypothesis that this transition largely involves interactions of the 3′-end of L-21 Sca I.

The structural differences between L-21 Sca I and L-21 Nhe I were probed by chemical modification at 50 and 0 °C. Figure 8b highlights nucleotides whose reactivity at Watson–Crick pairing positions changes by at least two levels at 50 °C. None of the new strong hits involve nucleotides in the middle of a helix, suggesting the secondary structures of the two molecules are the same. Comparison with Figure 8a, however, indicates there is considerable overlap with differences observed between L-21 Sca I at 65 and 50 °C. Six of the seven newly strong hits observed when L-21 Sca I is truncated to L-21 Nhe I are also positions of increased modification when the temperature of L-21 Sca I is raised

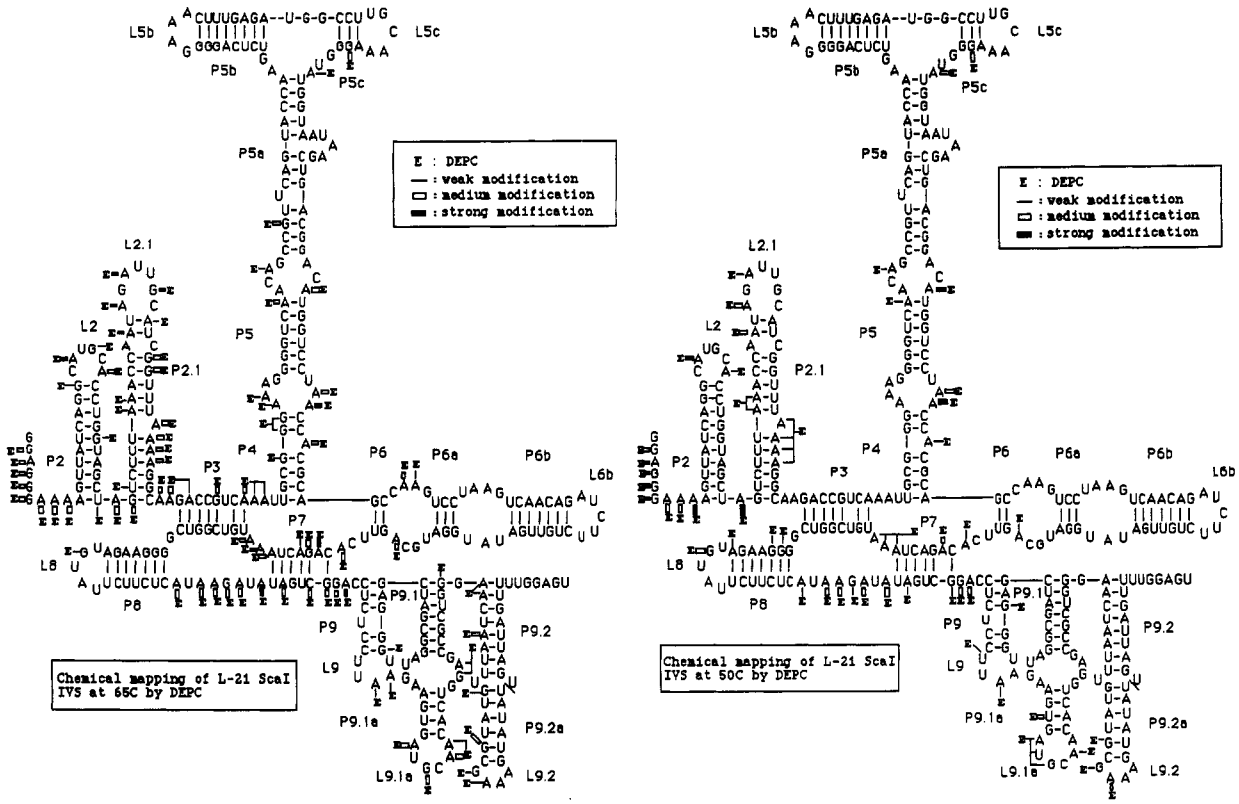

FIGURE 5: Chemical probing of the N7 positions of L-21 Sca I with DEPC (E) in melting buffer at (a, left) 65 °C and (b, right) 50 °C. Symbols show strong (solid rectangles), medium (open rectangles), and weak (—) modification.

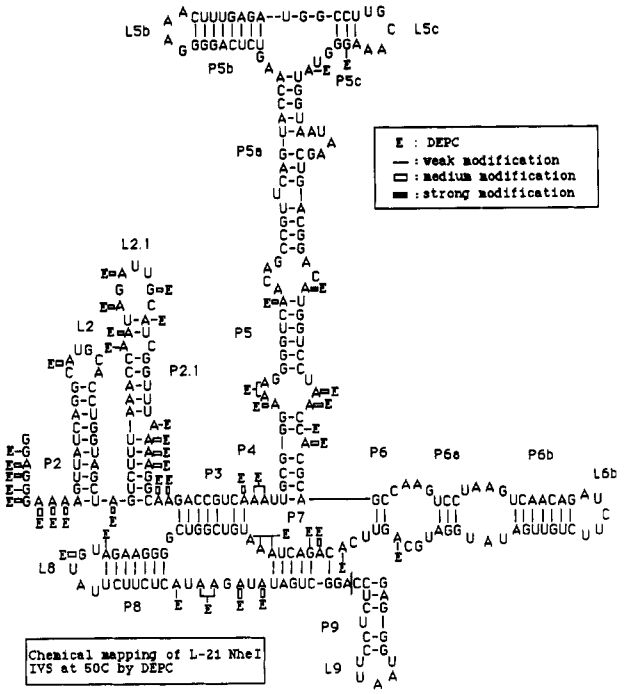

FIGURE 6: Chemical probing of the N7 positions of L-21 Nhe I with DEPC (E) in melting buffer at 50 °C. Symbols show strong (solid rectangles), medium (open rectangles), and weak (—) modification.

from 50 to 65 °C. Conversely, for nucleotides probed in all cases, six of 16 newly strong hits observed when L-21 Sca I is heated to 65 °C are also positions of increased reactivity when L-21 Sca I is truncated to Nhe I. Evidently, similar effects on structure are induced by heating L-21 Sca I from 50 to 65 °C and by deletion of the 3′-end of L-21 Sca I. This suggests tertiary interactions involving the 3′-end.

A similar picture emerges when L-21 Sca I and L-21 Nhe I are compared at 0 °C, although many of the nucleotides with altered reactivity are different (see supplementary material). Of the 10 nucleotides whose reactivity changes by at least 2 orders to give strong hits in L-21 Nhe I, none is in the middle of a helix. Seven are moderately or strongly modified in L-21 Sca I at 65 °C. This is also consistent with both truncation and the initial melting transition affecting tertiary rather than secondary structure.

Consideration of DEPC reactivity at N7 positions of purines is also consistent with similar effects being induced by heating of L-21 Sca I to 65 °C or truncation to L-21 Nhe I (Figures 5 and 6). Upon truncation, new moderate hits are observed at G77, A94, A95, A103, and A113. Except for A113, all are also newly reactive when L-21 Sca I is heated to 65 °C (see Figure 9).

The most likely tertiary interactions involve the loop L9.1a interacting with either loop L2 or L2.1 (Barfod & Cech, 1988). There are four potential pairing interactions with L2 and 12 with L2.1. In L-21 Sca I, all three loops are more strongly modified at 65 than 50 °C. Moreover, at both 50 and 0 °C, L2 and L2.1 are more strongly modified in L-21 Nhe I than in L-21 Sca I.

Phylogenetic comparison of sequences has been the most successful approach for identifying interactions in RNA (Michel & Westhof, 1990; Gutell et al., 1986; Pace et al., 1986). The hairpin loops, L2, L2.1, and L9.1a are not found in all group I introns and are therefore presumably not essential for function (Cech, 1988). Group I introns containing L9.1 and at least one of L2 and L2.1 are listed in Table II. To determine if the possible interaction between L9.1 and either L2 or L2.1 is also possible in other group I introns, we searched for complementarity between these regions. The potential pairings are shown in Table II. All the introns have possibilities for pairing between these regions, although the exact positions of the pairings are not conserved. Thus the phylogenetic data are consistent with a possible tertiary interaction between

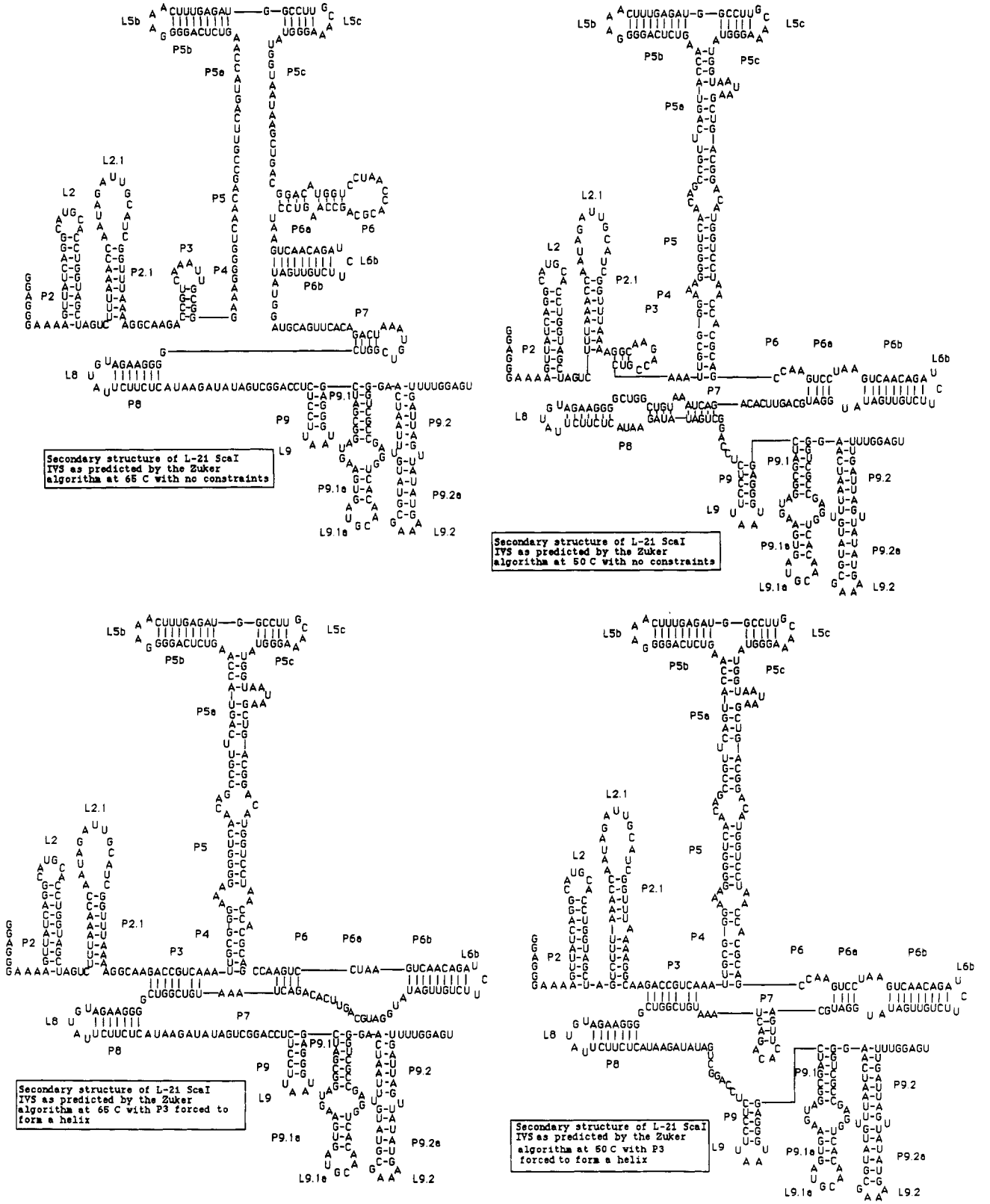

FIGURE 7: Computer predictions of secondary structure of L-21 Sca I using the program of Zuker (1989) and Jaeger et al. (1990a,b). Predicted structure with no constraints at (a, top left) 65 °C and (b, top right) 50 °C, and with seven base pairs of P3 forced at (c, bottom left) 65 °C and (d, bottom right) 50 °C.

these regions but do not prove its existence. Interestingly, all the pairings are rich in weak AU pairs, suggesting that any tertiary interaction may have dynamic character. Presumably, site-directed mutagenesis could be used to test the proposed tertiary interaction and to explore its functional significance.

The Mg^{2+} dependence of the L-21 Sca I transition with the lowest melting temperature is also consistent with a transition involving tertiary interactions. For tertiary interactions, the T_M is expected to be sensitive to Mg^{2+} concentration. For L-21 Sca I, reducing the Mg^{2+} from 10 to 1 mM in the presence of 50 mM Na^+ lowers the T_M of the first transition by about 12 °C (Figure 1c). This is more than double the effect expected for duplex formation by poly(A)·poly(U) in 64 mM Na^+ (Krakauer, 1974) or by dGCATGC at 50 mM Na^+ (Williams

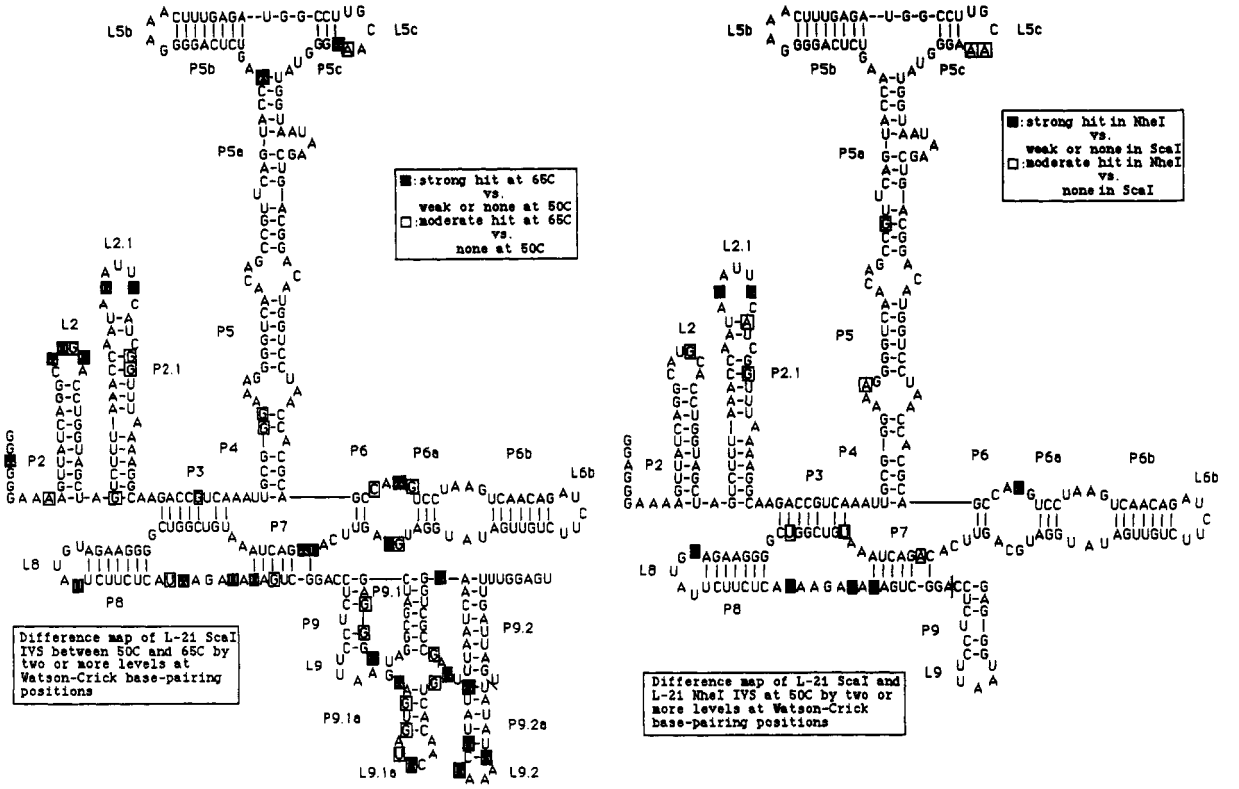

FIGURE 8: Comparison of chemical modification data of ribozymes at different temperatures at Watson–Crick base pairing positions. Differences shown are at least 2 orders (for example, weak vs strong modification). (a, left) Differences between modification maps of L-21 Sca I probed at 65 and 50 °C. A solid square represents a strong hit at 65 °C vs a weak or no hit at 50 °C. A hollow square represents a moderate hit at 65 °C vs no hit at 50 °C. (b, right) Differences between modification maps of L-21 Sca I and L-21 Nhe I at 50 °C. A solid square represents a strong hit in L-21 Nhe I vs a weak or no hit in L-21 Sca I. A hollow square represents a moderate hit in L-21 Nhe I vs no hit in L-21 Sca I.

et al., 1989). It is similar, however, to the 14 °C change in T_M observed between 1 and 10 mM Mg^{2+} for melting of tertiary structure in tRNA at 174 mM Na^+ (Cole et al., 1972). The melting curves of L-21 Sca I are consistent with the Fe(II)–EDTA cleavage results of Celander and Cech (1991). They observed that L-21 Sca I starts to unfold above 22 °C in the presence of 0.75 mM Mg^{2+} but persists to 45 °C with 1.5 mM Mg^{2+}. In Figure 1c, the first transition starts at about 40 °C in the presence of 1 mM free Mg^{2+}. Interestingly, the higher temperature transition in L-21 Sca I at 10 mM Mg^{2+} splits into at least two transitions at 1 mM Mg^{2+}, and all transitions appear less cooperative. This suggests that additional stages of folding can be elucidated from studies at low Mg^{2+} concentrations.

The conclusion that the low-temperature transition in L-21 Sca I melting is primarily due to disruption of tertiary interactions implies that the tertiary interactions are weaker than the secondary structure interactions. Similar conclusions were derived for melting of tRNAs (Crothers et al., 1974; Riesner & Römer, 1973; Hilbers et al., 1976). If this result is general, it suggests that a combination of melting and modification experiments may be useful for determining RNA structure. In particular, chemical modification experiments in the middle of the first transition can be used to limit possible secondary structures. For example, these constraints can be used to pick out reasonable secondary structures from a set generated by folding algorithms (Steger et al., 1984; Zuker, 1989; Zuker et al., 1991). In the L-21 Sca I case studied here, 47 strong hits are observed at 65 °C. This constrains the possible secondary structure much more than the 10 strong hits observed at 50 °C. Once the secondary structure is determined, differences in modification induced by lowering temperature can be used to infer tertiary interactions and

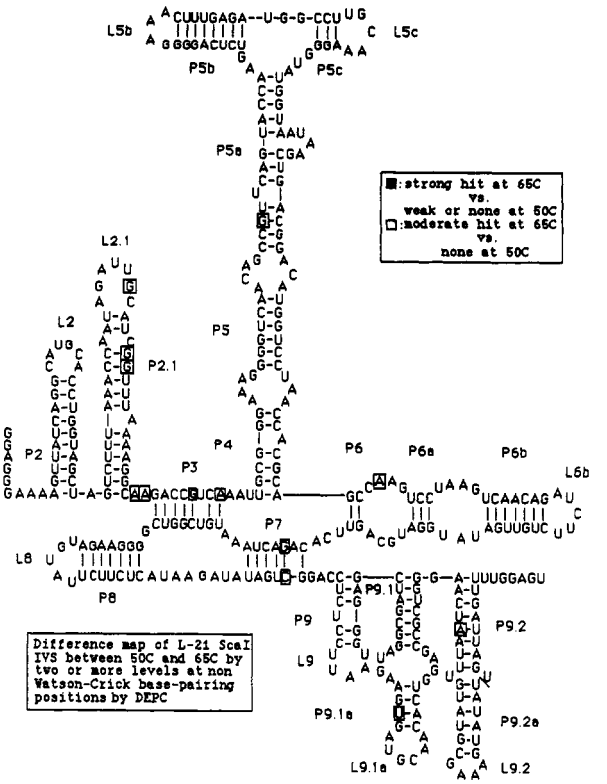

FIGURE 9: Comparison of chemical modification data probing N7 positions of L-21 Sca I with DEPC at 65 and 50 °C. A hollow square represents a moderate hit at 65 °C vs no hit at 50 °C. A similar difference map between L-21 Sca I and L-21 Nhe I at 50 °C shows moderate hits in L-21 Nhe I vs no hit in L-21 Sca I at G77, A94, A95, A103, and A113.

Table II. Complementary Sequences in P2 or P2.1 and P9.1 Regions That May Form Tertiary Pairs (Michel & Westhof, 1990 and references therein)

sequence	region	complementary nucleotides
Tt.LSU	P2.1	5'UUGCAUCG^{G}UUUA3'
	P9.1a	3'AACGUAGU$_{G}$AAGU5'
Tp.LSU	P2.1	5'UUGCAUCG^{G}UUU3'
	P9.1a	3'AACGUGGU$_{G}$AAG5'
Pp.LSU,1	P2.1	5'AAAAAAA3'
	P9.1	3'UUUUUUU5'
Pa.OX1,16	P2	5'AAU^{U}UAAUAUAG3'
	P9.1	3'UUA$_{U}$AUUAUAUU5'
Cp.tLeu	P2	5'UUAA3'
	P9.1	3'AAUU5'
Mp.tLeu	P2	5'UG^{A}GA3'
	P9.1	3'AU$_{G}$UU5'
Vf.tLeu	P2	5'UGGAA3'
	P9.1	3'AUUUU5'
Nt.tLeu	P2	5'AAA^{C}UU3'
	P9.1	3'UUU$_{A}$AA5'
Zm.tLeu	P2	5'UGGAAA3'
	P9.1	3'AUCUUU5'
Pa.OX1,3	P2	5'AUUCUU3'
	P9.1	3'UAGGAA5'
Pa.OX1,2	P2	5'GUAAU3'
	P9.1	3'CAUUA5'
Pa.ND5,3	P2	5'UA^{G}GA3'
	P9.1	3'AU$_{G}$UU5'
Ce.LSU,3	P2	5'UGAGU^{A}UU3'
	P9.1	3'AUUCG$_{A}$AA5'
Ce.LSU,4	P2	5'CUAA^{U}G3'
	P9.1	3'GGUU$_{U}$C5'
Sc.LSU	P2.1	5'UAUUG^{A}AA3'
	P9.1	3'AUAGC$_{A}$UU5'
Kt.LSU	P2.1	5'UAUUG^{A}AA3'
	P9.1	3'AUAGC$_{A}$UU5'
Kf.ATP9	P2.1	5'AUAUAAUA^{A}UA3'
	P9.1	3'UGUAUUAU$_{A}$AU5'
Sc.COB,5	P2	5'UCUUA3'
	P9.1	3'AGAAU5'
Nc.COB,2	P2	5'GUAG^{G}GUUUAAU3'
	P9.1	3'UAUU$_{A}$UAAAUUG5'
An.LSU	P2	5'UAUA3'
	P9.1	3'AUGU5'
Pa.LSU,1	P2	5'UAUUAA3'
	P9.1	3'AUAAUU5'
Pa.ND1,3	P2	5'UUGUAGAAAC3'
	P9.1	3'AGCAUUUUUG5'
Pa.OX2,2	P2	5'UAAUC^{C}UUGU3'
	P9.1	3'AUUAG$_{A}$AAUA5'
T4.nrdB	P2	5'UUUAU3'
	P9.1	3'GAAUA5'
Cm.psbA,1	P2	5'UAGAAAUA3'
	P9.1	3'AUCUUUGU5'
An.COB	P2	5'AAUG^{C}GG3'
	P9.1	3'UUAU$_{A}$UU5'
Cd.LUS,2	P2	5'UUUUA3'
	P9.1	3'AAAAU5'
T4.td	P2	5'UUAUA3'
	P9.1	3'AAUAU5'
Cr.LSU	P2	5'UGUAAG3'
	P9.1	3'GCAUUU5'

burial of residues. This information then provides constraints on the three-dimensional folding (Kim & Cech, 1987). The study presented here describes the process for unfolding induced by temperature. Unfolding induced by other variables, such as Mg^{2+} (Celander & Cech, 1991) or denaturant concentration, could provde similar or complementary information.

Comparison with Computer Predictions. There is one major disagreement between the chemical modification results and computer predictions of structures. At 65 °C, the folding algorithm (Zuker, 1989; Jaeger et al., 1989, 1990a,b) predicts the P3, P4, P5, and P5a helixes will be broken (see Figure 7a). Strong and moderate modification of 13 base-paired nucleotides is observed in this region, suggesting partial opening of helixes. Only three moderate hits are observed at nucleotides not adjacent to helix disruptions, however. Thus, the chemical modification data are not consistent with the complete opening of this region predicted by the computer algorithm.

Current thermodynamic parameters for structure prediction may underestimate the stability of the P3 to P5a helixes because they underestimate the stability of P3. When P3 is forced to pair in the algorithm, P4, P5, and P5a also pair correctly (see Figure 7c). There are two reasons that the stability of P3 is probably underestimated. First, it closes a multibranched loop. The linear approximation for the stability of this loop as a function of unpaired nucleotides probably overestimates the destabilization associated with closing this loop (Jaeger et al., 1990a). Second, P3 is probably stabilized by coaxial stacking with P8. Coaxial stacking of P3 and P8 is a feature of three-dimensional models of this intron based on phylogenetic data (Kim & Cech, 1987; Michel & Westhof, 1990). A similar motif with coaxial stacking of helixes separated by a GA mismatch is also observed in the crystal structure of phenylalanine tRNA (Kim et al., 1974; Robertus et al., 1974). Preliminary thermodynamic measurements on model systems indicate coaxial stacking can stabilize helixes (A. Walter, R. Kierzek, P. Müller, and D. H. Turner, unpublished observations), and preliminary incorporation of this effect in the structure prediction algorithm improves predictions of secondary structure (J. Kim, P. Müller, D. H. Turner, and M. Zuker, unpublished observations).

ACKNOWLEDGMENT

We thank Upjohn Company for their kind gift of kethoxal. We also thank R. Kierzek for sharing his unlimited knowledge on the chemistry of reactivities of the modification reagents with monomers.

SUPPLEMENTARY MATERIAL AVAILABLE

Eight figures showing kinetic plots of reaction between modification reagents and monomers and six figures showing chemical modification results on ribozymes (14 pages). Ordering information is given on any current masthead page.

REFERENCES

Barfod, E. T., & Cech, T. R. (1988) *Genes Dev. 2*, 652–663.

Barone, A. D., Tang, J. Y., & Caruthers, M. H. (1984) *Nucleic Acids Res. 12*, 4051–4061.

Bass, B. L., & Weintraub, H. (1988) *Cell 55*, 1089–1098.

Beaucage, S. L., & Caruthers, M. H. (1981) *Tetrahedron Lett. 22*, 1859–1862.

Bevington, P. R. (1969) *Data Reduction and Error Analysis for the Physical Sciences*, 1st ed., McGraw-Hill, New York.

Burke, J. M., Belfort, M., Cech, T. R., Davies, R. W., Schweyen, R., Shub, D., Szostak, J. W., & Tabak, H. (1987) *Nucleic Acids Res. 15*, 7217–7221.
Cech, T. R. (1988) *Gene 73*, 259–271.
Celander, D. W., & Cech, T. R. (1991) *Science 251*, 401–407.
Cole, P. E., Yang, S. K., & Crothers, D. M. (1972) *Biochemistry 11*, 4358–4368.
Crothers, D. M., Cole, P. E., Hilbers, C. W., & Shulman, R. G. (1974) *J. Mol. Biol. 87*, 63–88.
Davanloo, P., Rosenberg, A. W., Dunn, J. J., & Studier, F. W. (1984) *Proc. Natl. Acad. Sci. U.S.A. 81*, 2035–2039.
de Bruijn, M. H. L., & Klug, A. (1983) *EMBO J. 2*, 1309–1321.
Ehresmann, C., Baudin, F., Mougel, M., Romby, P., Ebel, J. P., & Ehresmann, B. (1987) *Nucleic Acids Res. 15*, 9109–9128.
Freier, S. M., Kierzek, R., Jaeger, J. A., Sugimoto, N., Caruthers, M. H., Neilson, T., & Turner, D. H. (1986) *Proc. Natl. Acad. Sci. U.S.A. 83*, 9373–9377.
Girshovich, A. S., Grachev, M. A., & Obukhova, L. V. (1968) *Mol. Biol. 2*, 286–296.
Gutell, R., Noller, H. F., & Woese, C. R. (1986) *EMBO J. 5*, 1111–1113.
He, L., Kierzek, R., SantaLucia, J., Jr., Walter, A. E., & Turner, D. H. (1991) *Biochemistry 30*, 11124–11132.
Hilbers, C. W., Robillard, G. T., Shulman, R. G., Blake, R. D., Webb, P. K., Fresco, R., & Riesner, D. (1976) *Biochemistry 15*, 1874–1882.
Inoue, T., & Cech, T. R. (1985) *Proc. Natl. Acad. Sci. U.S.A. 82*, 648–652.
Jaeger, J. A. (1989) Ph.D. Thesis, University of Rochester, Rochester, NY.
Jaeger, J. A., Turner, D. H., & Zuker, M. (1989) *Proc. Natl. Acad. Sci. U.S.A. 86*, 7706–7710.
Jaeger, J. A., Zuker, M., & Turner, D. H. (1990a) *Biochemistry 29*, 10147–10158.
Jaeger, J. A., Turner, D. H., & Zuker, M. (1990b) *Methods Enzymol. 183*, 281–306.
Joyce, G. F., & Inoue, T. (1989) *Nucleic Acids Res. 17*, 711–722.
Kim, S.-H., & Cech, T. R. (1987) *Proc. Natl. Acad. Sci. U.S.A. 84*, 8788–8792.
Kim, S.-H., Suddath, F. L., Quigley, G. J., McPherson, A., Sussman, J. L., Wang, A. H. J., Seeman, N. C., & Rich, A. (1974) *Science 185*, 435–440.
Kjems, J., Olesen, S. O., & Garrett, R. A. (1985) *Biochemistry 24*, 241–250.
Krakauer, H. (1974) *Biochemistry 13*, 2579–2589.
Litt, M. (1969) *Biochemistry 8*, 3249–3253.
Litt, M., & Hancock, V. (1967) *Biochemistry 6*, 1848–1854.
Manning, G. S. (1978) *Q. Rev. Biophys. 11*, 179–246.
Matteuchi, M., & Caruthers, M. H. (1981) *J. Am. Chem. Soc. 103*, 3185–3191.
Michel, F., & Dujon, B. (1983) *EMBO J. 2*, 33–38.
Michel, F., & Westhof, E. (1990) *J. Mol. Biol. 216*, 585–610.
Mitsuya, H., Yarchoan, R., & Broder, S. (1990) *Science 249*, 1533–1544.
Moazed, D., Stern, S., & Noller, H. F. (1986) *J. Mol. Biol. 187*, 399–416.
Nussinov, R., Pieczenik, G., Griggs, J. R., & Kleitman, D. J. (1978) *SIAM J. Appl. Math. 35*, 68–82.
Olson, M., Hood, L., Cantor, C., & Botstein, D. (1989) *Science 245*, 1434–1435.
Pace, N. R., Olsen, G. J., & Woese, C. R. (1986) *Cell 45*, 325–326.
Peattie, D. A. (1979) *Proc. Natl. Acad. Sci. U.S.A. 76*, 1760–1764.
Peattie, D. A., & Gilbert, W. (1980) *Proc. Natl. Acad. Sci. U.S.A. 77*, 4679–4682.
Record, M. T., Jr., Anderson, C. F., & Lohman, T. M. (1978) *Q. Rev. Biophys. 11*, 103–178.
Rhodes, D. (1977) *Eur. J. Biochem. 81*, 91–101.
Richards, E. G. (1975) in *Handbook of Biochemistry and Molecular Biology*: *Nucleic Acids* (Fasman, C. D., Ed.) 3rd ed., Vol. I, p 597, CRC Press, Cleveland, OH.
Riesner, D. (1987) in *The Viroids* (Diener, T. O., Ed.) pp 63–98, Plenum, New York.
Riesner, D., & Römer, R. (1973) in *Physico-Chemical Properties of Nucleic Acids* (Duchesne, J., Ed.) Vol. 2, pp 237–318, Academic Press, New York.
Robertus, J. D., Ladner, J. E., Finch, J. T., Rhodes, D., Brown, R. S., Clark, B. F. C., & Klug, A. (1974) *Nature 250*, 546–551.
Steger, G., Hofmann, H., Förtsch, J., Gross, H. J., Randles, J. W., Sänger, H. L., & Riesner, D. (1984) *J. Biomol. Struct. Dyn. 2*, 739–1102.
Stephens, J. C., Cavanaugh, M. L., Gradie, M. I., Mador, M. L., & Kidd, K. K. (1990) *Science 250*, 237–244.
Stern, S., Weiser, B., & Noller, H. F. (1988) *J. Mol. Biol. 204*, 447–469.
Turner, D. H., Sugimoto, N., & Freier, S. M. (1988) *Annu. Rev. Biophys. Biophys. Chem. 17*, 167–192.
Uhlmann, E., & Peyman, A. (1990) *Chem. Rev. 90*, 543–584.
van Belkum, A., Verlaan, P., Kun, J. B., Pleij, C., & Bosch, L. (1988) *Nucleic Acids Res. 16*, 1931–1950.
Williams, A. P., Longfellow, C. E., Freier, S. M., Kierzek, R., & Turner, D. H. (1989) *Biochemistry 28*, 4283–4291.
Wyatt, J. R., Puglisi, J. D., & Tinoco, I., Jr. (1990) *J. Mol. Biol. 214*, 455–470.
Zaug, A. J., Grosshans, C. A., & Cech, T. R. (1988) *Biochemistry 27*, 8924–8931.
Zuker, M. (1989) *Science 244*, 48–52.
Zuker, M., & Sankoff, D. (1984) *Bull. Math. Biol. 46*, 591–621.
Zuker, M., Jaeger, J. A., & Turner, D. H. (1991) *Nucleic Acids Res. 19*, 2707–2714.